THE ASTROPHYSICAL JOURNAL, 457:355–362, 1996 January 20

LAYERED ACCRETION IN T TAURI DISKS

CHARLES F. GAMMIE
Center for Astrophysics, MS-51, 60 Garden Street, Cambridge, MA 02138
Received 1995 May 8; accepted 1995 July 28

ABSTRACT

We put forward a model for accretion disks around T Tauri stars. The model assumes that angular momentum transport is driven by magnetic fields and can occur only in those parts of the disk that are sufficiently ionized that the gas can couple to the magnetic field. These regions lie at $R \lesssim 0.1$ AU, where collisional ionization is effective, and at $R \gtrsim 0.1$ AU in a layer of thickness ≈ 100 g cm^{-2} at the surface of the disk where cosmic-ray ionization is effective.

The model predicts that the stellar accretion rate is about $10^{-8}\ M_\odot\ \mathrm{yr}^{-1}$, independent of the rate of infall onto the disk. Matter that is not accreted onto the star accumulates in the inner few AU of the disk at a rate of about $10^{-3}\ M_\odot$ in 10^4 yr. Given this buildup it is unlikely that accretion is steady. The effective temperature profile is $T_e \sim r^{-1/2}$ outside of 0.1 AU, which differs from the canonical $T_e \sim r^{-3/4}$. We calculate the expected spectral energy distribution for the disk and show that this temperature profile produces an infrared excess. Finally, we discuss some of the leading uncertainties in the theory.

Subject headings: accretion, accretion disks — stars: magnetic fields — stars: pre–main-sequence

1. INTRODUCTION

The origin of angular momentum transport in accretion disks remains one of the central problems of accretion disk theory. Recently, progress has been made with the discovery of a weak-field magnetohydrodynamic (MHD) instability in differentially rotating disks by Balbus & Hawley (1991, hereafter BH). This instability sets in under a broad range of conditions and is capable of initiating and sustaining MHD turbulence in disks. Numerical simulations demonstrate that the turbulence initiated by the instability transports significant angular momentum (Hawley, Gammie, & Balbus 1995a, hereafter HGB1) and can sustain a disordered magnetic field in the presence of dissipation (Hawley, Gammie, & Balbus 1995b, hereafter HGB2; Brandenburg et al. 1995). The success of this theory of angular momentum transport in disks suggests that we should consider seriously the implications of magnetically driven transport in disks of various types.

Disks around T Tauri stars, in particular, are likely to be very cold and dense. As a consequence recombination is rapid, and the number density of free electrons is small: the gas in orbit about young stars is, by astrophysical standards, an exceptionally poor conductor of electrical currents (Hayashi 1981). When the conductivity is low enough, the disk gas decouples from the magnetic field and is linearly stable to the BH modes. If turbulence initiated by the BH instability is the dominant angular momentum transport mechanism, then those parts of the disk that are decoupled from the field should be quiescent.

One might simply accept the low conductivity of T Tauri disks as evidence for the importance of a nonmagnetic angular momentum transport mechanism, such as convection (Paczyński 1976; Cameron 1978; Lin & Papaloizou 1980) or nonlinear hydrodynamic instability (Shakura, Sunyaev, & Zilitinkevich 1978; more recently Zahn 1991; Dubrulle 1992). However, these mechanisms have run into serious theoretical difficulties (see Ryu & Goodman 1992 and Stone & Balbus 1995 for the case against convective angular momentum transport, and Balbus, Hawley, & Stone 1995 for a discussion of nonlinear hydrodynamic instability) that can be traced to the strongly stabilizing influence of the Coriolis force. While other nonmagnetic angular momentum transport mechanisms, such as gravitational instability, are undoubtedly effective and potentially important in the outer parts of T Tauri disks, it seems more fruitful to ask if accretion might not proceed only in those parts of the disk that are coupled to the field.

Which parts of disks around T Tauri stars are well coupled to the magnetic field? In § 2 we consider ionization equilibrium in T Tauri disks. We show that inside some critical radius R_c the field is well coupled to the gas because of collisional ionization. Outside R_c a layer of approximately constant surface density Σ_a near the surface of the disk is ionized by cosmic rays; sandwiched between these "active" layers is a "dead" layer that is decoupled from the field. Equipped with these estimates for the location of the active and dead zones, we construct a model for T Tauri disks in § 3. The model is remarkably predictive and allows us to calculate the accretion rate onto the central star. The accretion rate is limited because the accretion flow is restricted to the active layer. In this sense the active layer acts as a gate, allowing only a fraction of the mass flux available at large radius onto the central star. Significant uncertainties remain in the model, but also good prospects for improvement and further development. These are discussed in § 4.

2. RESISTIVITY AND IONIZATION EQUILIBRIUM

Resistive dissipation, rather than ambipolar diffusion, is likely to be the leading source of magnetic field diffusion in most parts of T Tauri disks (Hayashi 1981). The magnetic resistivity η appears in the induction equation as

$$\frac{\partial \boldsymbol{B}}{\partial t} = \nabla \times (\boldsymbol{v} \times \boldsymbol{B}) - \nabla \times (\eta \nabla \times \boldsymbol{B})\,. \tag{1}$$

The resistivity is related to electron fraction $x \equiv n_e/n_{\mathrm{H}}$ via

$$\eta = 6.5 \times 10^3 x^{-1}\ \mathrm{cm}^2\ \mathrm{s}^{-1} \tag{2}$$

(Hayashi 1981), if electrons are the main current carriers. This is true if, as we shall assume, there are few small grains.

A large enough resistivity can suppress the linear instability of BH. At a scale λ, the instability is suppressed if the growth rate of the instability in the absence of resistivity, which is, in the weak-field limit, V_A/λ [$V_A \equiv B/(4\pi\rho)^{1/2}$ is the Alfvén speed], is smaller than the resistive damping rate, $\sim\eta/\lambda^2$. Clearly, the larger the scale, the larger the resistivity that is required to suppress the instability. But the largest available scale is the scale height $H = c_s/\Omega$ [here c_s is the sound speed and $\Omega = (GM/R^3)^{1/2}$ is the Keplerian rotation frequency]; larger scale modes will not fit within the disk. Therefore the instability is suppressed when $\eta \gtrsim V_A H$.

In order to decide when the instability is suppressed, then, we need to know the field strength. Numerical simulations (HGB1, HGB2) show that the shear stress $w_{r\phi}$ due to turbulence induced by the instability is $w_{r\phi} \simeq \rho V_A^2$. If we express the shear stress in terms of the α parameter of Shakura & Sunyaev (1973), $w_{r\phi} = \alpha\rho c_s^2$, then we have $V_A \simeq \alpha^{1/2} c_s$. We can now define a magnetic Reynolds number,

$$Re_M \equiv \frac{V_A H}{\eta} = 7.4 \times 10^{13} x \alpha^{1/2} \left(\frac{R}{1\ \mathrm{AU}}\right)^{3/2} \left(\frac{T}{500\ \mathrm{K}}\right) \left(\frac{M}{M_\odot}\right)^{-1/2} . \quad (3)$$

The instability will be suppressed if $Re_M \lesssim 1$; we are implicitly assuming that this is also the condition for the decay of BH-instability induced turbulence. Since most of the terms in parentheses, and $\alpha^{1/2}$, are likely to be within an order of magnitude of unity, the magnetic field will be well coupled to the gas when $x \gtrsim 10^{-13}$.

Umebayashi (1983) has calculated x as a function of temperature and density assuming complete chemical equilibrium. He finds that, at a density $n_H = 10^{13}$ (x depends only logarithmically on density), x rises from about 10^{-16} at 800 K to 10^{-13} at 900 K to 10^{-11} at 10^3 K. This rapid increase in x is almost entirely due to the collisional ionization of potassium. Since x depends nearly exponentially on temperature, while the other factors entering the magnetic Reynolds number vary only weakly with temperature, we shall make the approximation that for $T > 10^3$ K the gas is well coupled to the magnetic field.

At those radii where collisional ionization is ineffective ($T < 10^3$ K), cosmic-ray ionization dominates.[1] Cosmic rays have an interstellar ionization rate $\zeta \simeq 10^{-17}$ s^{-1} (Spitzer & Tomasko 1968). They enter the disk from the top and the bottom and are attenuated exponentially by the disk material with a stopping depth of $\Sigma_0 \approx 10^2$ g cm^{-2} (Umebayashi & Nakano 1981).[2] We shall make the approximation that a layer of surface density Σ_a near the top of the disk is active, while the material at greater depth, of surface density Σ_d, is poorly coupled to the field; the approximation consists of taking the transition to be sharp when it is likely to be spread out over as much as a scale height. While the active column Σ_a can be smaller than Σ_0, it cannot be much larger, because below Σ_0 the cosmic-ray flux drops exponentially with depth. We make the further approximation that $\Sigma_a \simeq \Sigma_0$; this is only valid, however, if $Re_M > 1$ at the base of the active layer.

An upper limit to the magnetic Reynolds number can be obtained as follows. In general, the electron fraction x will depend on the abundance of small grains; for a standard interstellar grain size spectrum (Mathis, Rumpl, & Nordsieck 1977) the small grains present a large cross section for collision with electrons and efficiently remove them from the gas phase at the densities characteristic of T Tauri disks (see the comprehensive discussion of Umebayashi 1983 for all the relevant recombination pathways). A large recombination rate will decouple the gas from the field, and, by hypothesis, leave the gas quiescent. If the gas is quiescent, then the grain size spectrum will evolve, and large grains will precipitate toward the midplane of the disk (e.g., Weidenschilling & Cuzzi 1993). The recombination rate should then decline, raising the electron fraction toward a level that couples the gas with the field.

While a reduction in grain-surface recombination can lower the recombination rate, it cannot lower it below the gas-phase recombination rate, which is $\beta n_H^2 x^2$. A typical recombination coefficient, due to dissociative recombination, is $\beta \simeq 8.7 \times 10^{-6} T^{-1/2}$ cm^3 s^{-1} (Glassgold, Lucas, & Omont 1986). Then an upper limit on the electron fraction is

$$x = \left(\frac{\zeta}{\beta n_H}\right)^{1/2} = 1.6 \times 10^{-12} \left(\frac{T}{500\ \mathrm{K}}\right)^{1/4} \times \left(\frac{\zeta}{10^{-17}\ \mathrm{s}^{-1}}\right)^{1/2} \left(\frac{n_H}{10^{13}\ \mathrm{cm}^{-3}}\right)^{-1/2} . \quad (4)$$

Substituting into equation (3), we see that the condition that the top layer of the disk is sufficiently ionized is marginally satisfied for temperatures and densities comparable to those in T Tauri disks. This condition can be checked more carefully once a disk model is formulated, but we are encouraged to provisionally accept the approximation $\Sigma_a \simeq \Sigma_0$.

A large uncertainty in this calculation is the cosmic-ray ionization rate at the surface of the disk, ζ. In the present-day solar system the flux of galactic cosmic rays is reduced from its interstellar value because of diffusion, convection, drift, and adiabatic cooling in the solar wind (see Jokipii 1991). T Tauri stars, of course, have powerful winds, which may shield the accretion disk from galactic cosmic rays. Cosmic-ray transport in T Tauri winds is likely to be rather different from transport in the solar wind, however, since T Tauri winds are denser, have stronger magnetic fields, and exhibit greater variation with stellar latitude than the solar wind. An additional source of ionization may be relativistic protons accelerated in flares located in the T Tauri star's corona or in the disk's corona. While the Sun is a weak source of relativistic protons, X-ray and radio continuum observations of T Tauri stars indicate that they are much more active than the Sun (see the review of Montmerle et al. 1993), so it is likely that they produce more relativistic protons than the Sun; whether this flux is comparable to the galactic flux at any point in the disk is not clear. Both shielding of the disk by the T Tauri wind and production of relativistic protons by the star-disk system may be important, but we cannot evaluate the amplitude of these effects with any confidence. In the absence of better information we shall simply set ζ to its presumed interstellar value of 10^{-17} s^{-1} (Spitzer & Tomasko 1968).

[1] The ionization rates due to the decay of ^{40}K, and ^{26}Al if it is present and uniformly distributed with an abundance of 5×10^{-5} relative to ^{27}Al, are lower than the interstellar cosmic-ray ionization rate by about 6 orders of magnitude, and 2 orders of magnitude, respectively (see Stepinski 1992).

[2] Dolginov & Stepinski (1994) have argued that cosmic rays will not penetrate even to this depth, because the cosmic rays must travel along a tangled magnetic field. The penetration depth is then of order $(\Sigma_0 \Lambda)^{1/2}$, where Λ is the column corresponding to the characteristic scale of the field. In numerical simulations of BH-instability induced turbulence (HGB1), however, nearly all the field energy is concentrated in the largest scale Fourier components, with characteristic scale of order H, so the penetration depth should be of order Σ_0.

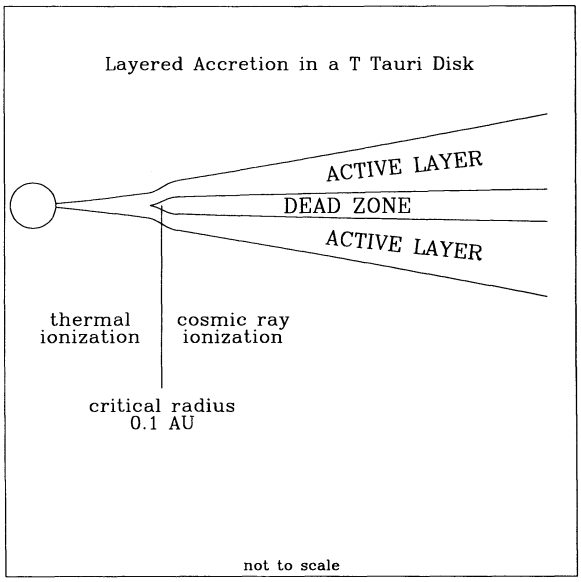

FIG. 1.—Sketch showing the key features of a layered accretion disk. Inside $\simeq 0.1$ AU, where $T \simeq 10^3$ K, collisional ionization is sufficient to couple the magnetic field to the gas. Outside this critical radius cosmic rays ionize a layer of thickness $\simeq 100$ g cm^{-2} on either side of the disk. Sandwiched between these active layers is a dead zone where no accretion occurs.

A graphical summary of the structure of magnetically driven low-ionization disks is given in Figure 1. From the accreting star out to the critical radius R_c, where $T < 10^3$ K, the entire disk is coupled to the field because collisional ionization of alkali metals is effective. At larger radii the disk has an active layer near the surface where cosmic-ray ionization is effective, and a dead zone near the midplane. The dead zone will come into thermal equilibrium with the base of the active layer (and hence be isothermal) provided there is no dissipation within the dead zone. Settling of solids to the midplane could complicate the structure of the dead zone in an interesting way, but in what follows we shall simply assume that it is isothermal. At still larger radii (not shown in Fig. 1) the disk will become sufficiently thin that cosmic rays penetrate the entire disk and the layered structure will disappear, giving way to a more conventional structure in which the entire disk is turbulent.

3. DISK MODEL

We shall now construct a model for a T Tauri disk assuming that angular momentum transport is allowed only in the active layers.

We shall assume that angular momentum transport is entirely internal to the disk, that is, that MHD winds do not carry off a significant amount of angular momentum (although coupling of the MHD wind to the disk is also limited to the active layers outside R_c; see the discussion of Königl 1995). We shall also assume that transport is entirely due to MHD turbulence, so that any transport due to convection-induced turbulence is neglected. To the extent that simulations of the nonlinear outcome of the BH instability give a prescription for treating angular momentum transport, they are consistent with the α-viscosity prescription of Shakura & Sunyaev (1973), with an effective viscosity $\nu = \alpha c_s H$ and $\alpha \sim 10^{-2}$ (HGB1; HGB2). We adopt the α prescription, but we will scale α to 10^{-2} in our solutions.

Assuming the effective viscosity is present only in the active layers, the azimuthal component of the momentum equation gives a familiar expression for the inward mass flux $\dot{M}(r)$ at radius r:

$$\dot{M} = 6\pi r^{1/2} \frac{\partial}{\partial r} (2\Sigma_a \nu r^{1/2}) . \tag{5}$$

Here $2\Sigma_a$ is the (constant) total surface density of the active layers.

Energy balance requires that the energy deposited by viscous dissipation in each active layer is equal to the energy radiated away at each surface of the disk, giving

$$\tfrac{9}{4}\Sigma_a \nu \Omega^2 = \sigma T_e^4 , \tag{6}$$

where T_e is the effective temperature of the disk and the other symbols have their usual meanings. Furthermore, we assume that the vertical transport of energy is governed by radiative diffusion, giving

$$T_c^4 \simeq \tfrac{3}{8}\tau T_e^4 \tag{7}$$

(Hubeny 1990). Here $\tau = \Sigma_a \kappa$ is the optical depth, T_c is the central temperature, and $\kappa(\rho, T)$ is the Rosseland mean opacity.

For the opacities, we use the analytic approximations provided by Bell & Lin (1994). Three opacities regimes are of interest to us here. Between $2290\rho^{2/49}$ K and 203 K the opacity is dominated by grains composed of iron and silicates, and $\kappa = 0.1T^{1/2}$ cm^2 g^{-1}. Between 203 K and 167 K water condenses into solid form and the opacity is $\kappa = 2 \times 10^{16} T^{-7}$ cm^2 g^{-1}. Below 167 K water vapor is absent, water ice grains dominate the opacity, and $\kappa = 2 \times 10^{-4} T^2$. Transitions between opacity regimes are taken to be sudden. In nature these transitions will be smoother, but this would have no effect on our solutions except to smooth the transitions between opacity zones.

The opacities have been calculated with an assumed grain size spectrum (see Pollack, McKay, & Christofferson 1985); our assumption in using gas-phase recombination rates rather than grain surface recombination rates is that the dust grain size spectrum has evolved so that there are far fewer small grains. Pollack et al. (1985) have considered the effects of varying grain size spectra on the opacity in these regimes. There are two important effects, which are best described in terms of a dust grain of that radius which contributes most to the opacity. First, the size of this typical grain can evolve. For a fixed mass density in grains of the typical size, the opacity is largest when this size matches the local thermal wavelength of light. Thus, if the grains are initially small, the opacity can increase as grains coagulate. Second, the number density of these typical grains can become smaller, thereby reducing the opacity, if a large part of the total grain mass is locked up in large grains that do not contribute to the opacity. In sum, the opacities depend on the evolution of the grain size spectra and are therefore uncertain. As an indicator of how sensitive our results are to variations in the opacity, we multiply all opacities by a dummy constant κ_0 and exhibit the κ_0 dependence in our solutions.

The only remaining piece of physics to be specified is the vertical hydrostatic equilibrium. If the dead zone column is zero, then

$$H = c_s/\Omega , \tag{8}$$

where as usual H is the scale height. As the dead zone column increases, however, the active layers will be forced away from the midplane of the disk. Since the gravitational acceleration increases away from the midplane, the scale height will be reduced somewhat as Σ_d increases. This effect is noticeable only if $\Sigma_d \gg \Sigma_a$;[3] we shall use equation (8) throughout.

We can now solve for the disk structure in those regions where the disk is divided into active and dead layers. In the silicate-iron grain opacity regime, using equations (5), (6), (7), and (8), we obtain for the active layer,

$$T_c = 290\left(\frac{r}{1\ \mathrm{AU}}\right)^{-3/5}\left(\frac{M}{1\ M_\odot}\right)^{1/5}\left(\frac{\alpha}{10^{-2}}\right)^{2/5} \times \left(\frac{\Sigma_a}{100\ \mathrm{g\ cm^{-2}}}\right)^{4/5}\kappa_0^{2/5}\ \mathrm{K}\ , \quad (9)$$

$$T_e = 102\left(\frac{r}{1\ \mathrm{AU}}\right)^{-21/40}\left(\frac{M}{1\ M_\odot}\right)^{7/40}\left(\frac{\alpha}{10^{-2}}\right)^{7/20} \times \left(\frac{\Sigma_a}{100\ \mathrm{g\ cm^{-2}}}\right)^{9/20}\kappa_0^{1/10}\ \mathrm{K}\ , \quad (10)$$

$$\dot{M} = 1.17\times 10^{-7}\left(\frac{r}{1\ \mathrm{AU}}\right)^{9/10}\left(\frac{M}{1\ M_\odot}\right)^{-3/10}\left(\frac{\alpha}{10^{-2}}\right)^{7/5} \times \left(\frac{\Sigma_a}{100\ \mathrm{g\ cm^{-2}}}\right)^{9/5}\kappa_0^{2/5}\ M_\odot\ \mathrm{yr}^{-1}\ , \quad (11)$$

$$\tau = 170\left(\frac{r}{1\ \mathrm{AU}}\right)^{-3/10}\left(\frac{M}{1\ M_\odot}\right)^{1/10}\left(\frac{\alpha}{10^{-2}}\right)^{1/5} \times \left(\frac{\Sigma_a}{100\ \mathrm{g\ cm^{-2}}}\right)^{7/5}\kappa_0^{6/5}\ , \quad (12)$$

$$\rho_c = 1.68\times 10^{-10}\left(\frac{r}{1\ \mathrm{AU}}\right)^{-6/5}\left(\frac{M}{1\ M_\odot}\right)^{2/5}\left(\frac{\alpha}{10^{-2}}\right)^{-1/5} \times \left(\frac{\Sigma_a}{100\ \mathrm{g\ cm^{-2}}}\right)^{3/5}\kappa_0^{-1/5}\ \mathrm{g\ cm^{-3}}\ , \quad (13)$$

$$\frac{H}{r} = 0.0396\left(\frac{r}{1\ \mathrm{AU}}\right)^{1/5}\left(\frac{M}{1\ M_\odot}\right)^{-2/5}\left(\frac{\alpha}{10^{-2}}\right)^{1/5} \times \left(\frac{\Sigma_a}{100\ \mathrm{g\ cm^{-2}}}\right)^{2/5}\kappa_0^{1/5}\ , \quad (14)$$

$$\frac{\Omega r}{v_r} = 15{,}200\left(\frac{r}{1\ \mathrm{AU}}\right)^{-2/5}\left(\frac{M}{1\ M_\odot}\right)^{4/5} \times \left(\frac{\alpha}{10^{-2}}\right)^{-7/5}\left(\frac{\Sigma_a}{100\ \mathrm{g\ cm^{-2}}}\right)^{-4/5}\kappa_0^{-2/5}\ , \quad (15)$$

$$P = 2.35\left(\frac{r}{1\ \mathrm{AU}}\right)^{-9/5}\left(\frac{M}{1\ M_\odot}\right)^{3/5}\left(\frac{\alpha}{10^{-2}}\right)^{1/5} \times \left(\frac{\Sigma_a}{100\ \mathrm{g\ cm^{-2}}}\right)^{7/5}\kappa_0^{1/5}\ \mathrm{g\ cm^{-1}\ s^{-2}}\ , \quad (16)$$

[3] In the limit that $\Sigma_d \gg \Sigma_a$, it can be shown that $H \sim c_s/\Omega[\ln(\Sigma_d/\Sigma_a)]^{1/2}$.

$$B \simeq \sqrt{8\pi\alpha P} = 0.768\left(\frac{r}{1\ \mathrm{AU}}\right)^{-9/10}\left(\frac{M}{1\ M_\odot}\right)^{3/10} \times \left(\frac{\alpha}{10^{-2}}\right)^{3/5}\left(\frac{\Sigma_a}{100\ \mathrm{g\ cm^{-2}}}\right)^{7/10}\kappa_0^{1/10}\ \mathrm{G}\ . \quad (17)$$

Notice that this model is formally similar to the constant $\dot{M}$ disk model of Shakura & Sunyaev (1973), except that here the surface density is held fixed and $\dot{M}$ is allowed to vary with r.

It is important to check that the solution is self-consistent in the sense that the magnetic Reynolds number at the base of the active layer is large enough to couple the field to the gas. Combining equations (3), (4), (9), and (13),

$$Re_M = 0.54\left(\frac{r}{1\ \mathrm{AU}}\right)^{27/20}\left(\frac{M}{1\ M_\odot}\right)^{-9/20}\left(\frac{\alpha}{10^{-2}}\right)^{11/10} \times \left(\frac{\Sigma_a}{100\ \mathrm{g\ cm^{-2}}}\right)^{7/10}\kappa_0^{3/5} \quad (18)$$

This is consistent with a well-coupled field, given the uncertainties in Σ_a and α.

Equations (9)–(17) are valid so long as $T_c < 10^3$ K. At higher temperature potassium is collisionally ionized and the midplane of the disk becomes active. The central temperature rises above 10^3 K at a radius

$$R_c \equiv 0.13\left(\frac{M}{1\ M_\odot}\right)^{1/3}\left(\frac{\alpha}{10^{-2}}\right)^{2/3}\left(\frac{\Sigma_a}{100\ \mathrm{g\ cm^{-2}}}\right)^{4/3}\kappa_0^{2/3}\ \mathrm{AU}\ . \quad (19)$$

At this radius the accretion rate is

$$\dot{M} = 1.8\times 10^{-8}\left(\frac{\alpha}{10^{-2}}\right)^{2}\left(\frac{\Sigma_a}{100\ \mathrm{g\ cm^{-2}}}\right)^{3}\kappa_0\ M_\odot\ \mathrm{yr}^{-1}\ . \quad (20)$$

Inside R_c the entire disk is active, so the mass flux will be constant down to the stellar surface. Therefore, equation (20) gives the accretion rate in the inner disk and onto the star.[4] Notice that the accretion rate is rather sensitive to both Σ_a and α; since neither is known to great accuracy, the accretion rate is rather poorly constrained. Remarkably, however, our best estimates for α and Σ_a produce an accretion rate that lies within the range $10^{-8}\ M_\odot\ \mathrm{yr}^{-1}$ to a few times $10^{-7}\ M_\odot\ \mathrm{yr}^{-1}$ inferred from optical observations of T Tauri stars (Hartmann & Kenyon 1990; Basri & Bertout 1989).

The inward mass flux $\dot{M}$ is an increasing function of r in the active layer model. This implies that material accumulates in the dead zone; the accumulation rate per unit surface area is

$$\frac{\partial\Sigma_d}{\partial t} = \frac{1}{2\pi r}\frac{\partial\dot{M}}{\partial r} = 0.07\left(\frac{r}{1\ \mathrm{AU}}\right)^{-11/10}\left(\frac{M}{1\ M_\odot}\right)^{-3/10} \times \left(\frac{\alpha}{10^{-2}}\right)^{7/5}\left(\frac{\Sigma_a}{100\ \mathrm{g\ cm^{-2}}}\right)^{9/5}\kappa_0^{2/5}\ \mathrm{g\ cm^{-2}\ yr^{-1}}\ . \quad (21)$$

The total accumulation rate in the dead zone in the silicate-iron grain opacity regime ($T_c > 203$ K) is essentially the total mass flux at the outer edge of the opacity regime, since only a

[4] We have assumed that the mass flux is continuous from the layered solution at $R > R_c$ to the constant mass flux solution at $R < R_c$. This implies that the temperature is not continuous; it rises as one moves inward across R_c by a factor of $2.8^{1/4}$. In consequence radial radiative diffusion may move R_c outward somewhat. This will tend to increase the stellar accretion rate.

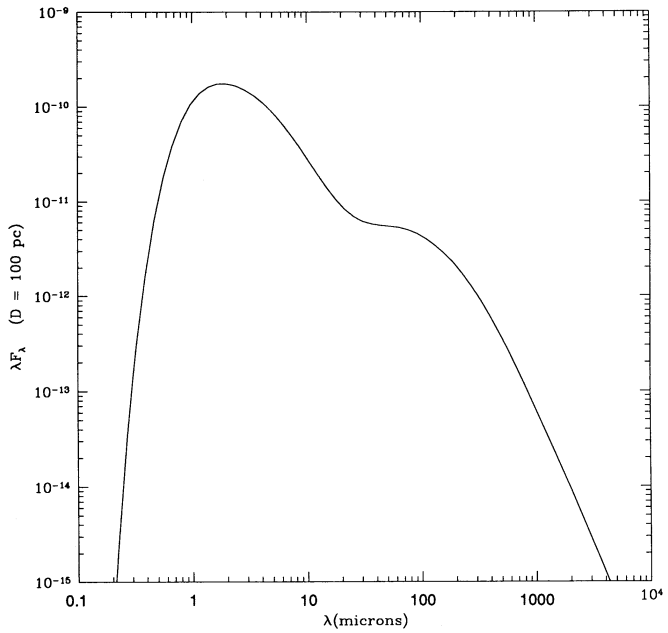

FIG. 2.—The spectral energy distribution of a layered accretion disk model, seen face-on at a distance of 100 pc. The star, boundary layer, and reprocessed light are not included. The disk extends from 2.5 $R_\odot$ to 28 AU. The spectrum is very nearly that of a standard steady state disk at $\lambda \lesssim 20$ μm; this piece of the spectrum is generated by the disk inside the critical radius. At longer wavelength λF_λ is flat; this piece of the spectrum is generated by the disk outside the critical radius, where $T_e \sim r^{-1/2}$.

small fraction of the mass makes it onto the star. Integrated over a time Δt, the mass deposited in the dead zone is

$$M_{dz} \simeq 1.3 \times 10^{-3}\left(\frac{\alpha}{10^{-2}}\right)^2\left(\frac{\Sigma_a}{100\ \mathrm{g\ cm^{-2}}}\right)^3\kappa_0\left(\frac{\Delta t}{10^4\ \mathrm{yr}}\right) M_\odot\ . \tag{22}$$

Additional mass will accumulate in the dead zone that lies in the water vapor and water ice opacity regimes.

The fact that material gradually accumulates in the dead zone strongly suggests that accretion cannot be time-steady in T Tauri disks. The dead zone is like a tinderbox, waiting to be ignited. Suppose some event raises the temperature of part of the dead zone above 10^3 K, thereby coupling it to the magnetic field and activating it. If a large enough reservoir of mass is present, accretion of that mass can sustain the elevated temperature, and the stellar accretion rate will be greatly enhanced. Such an event would bear some similarity to FU Orionis events (see the review of Hartmann, Kenyon, & Hartigan 1993) in which a few times 10^{-3} $M_\odot$ is accreted over the course of several decades.

The solutions for layered accretion in the ice sublimation and water ice opacity zones is given in the Appendix. It is natural to join the solutions together by requiring that the temperature be continuous where they join. This leads to the interesting feature that $\dot{M}(r)$ and v_r change discontinuously at the boundary between opacity regimes. This happens because $\dot{M}$ is proportional to a radial derivative of Σv, (see eq. [5]) and the slope of Σv changes rapidly at the opacity transition. As a result, material will either accumulate or be depleted from the transition region. The transition between grain and ice-sublimation opacities occurs near $T_c = 203$ K, which lies at a radius

$$R_{g-s} \equiv 1.8\left(\frac{M}{1\ M_\odot}\right)^{1/3}\left(\frac{\alpha}{10^{-2}}\right)^{2/3}\left(\frac{\Sigma_a}{100\ \mathrm{g\ cm^{-2}}}\right)^{4/3}\kappa_0^{2/3}\ \mathrm{AU}\ . \tag{23}$$

Subtracting the mass flux inside R_{g-s} from that outside, we find that mass will accumulate over a small range in radius at a rate

$$\Delta\dot{M} = 6.1 \times 10^{-8}\left(\frac{\alpha}{10^{-2}}\right)^2\left(\frac{\Sigma_a}{100\ \mathrm{g\ cm^{-2}}}\right)^3\kappa_0\ M_\odot\ \mathrm{yr}^{-1}\ . \tag{24}$$

About a quarter of the mass flux is deposited in the dead zone at R_{g-s}, while the rest continues inward. Since this large mass flux is deposited over a rather small area, there is the possibility of gravitational instability. If we assume the material is deposited over δ scale heights in radius and that the dead zone is initially empty, then the Toomre Q parameter ($Q < 1$ implies local gravitational instability of a thin disk) is

$$Q = 13\,\delta^{-1}\left(\frac{M}{1\ M_\odot}\right)^{1/3}\left(\frac{\alpha}{10^{-2}}\right)^{-4/3} \times\left(\frac{\Sigma_a}{100\ \mathrm{g\ cm^{-2}}}\right)^{-5/3}\kappa_0^{-1/3}\left(\frac{t}{10^4\ \mathrm{yr}}\right), \tag{25}$$

if the material is allowed to accumulate for time t. This produces instability after a rather short time interval. The Q criterion may be inappropriate, however, since the material will form a slender, self-gravitating annulus, which is subject to various global instabilities even when stable by the Q criterion (see Christodoulou & Narayan 1992). In any event, the onset of a dynamical instability at R_{g-s} could activate (heat to 10^3 K) material in the dead zone at smaller radius, causing an enhanced accretion event, similar to an FU Orionis outburst.

The transition between ice-sublimation and ice grain opacities, on the other hand, occurs at

$$R_{s-i} \equiv 6.6\left(\frac{M}{M_\odot}\right)^{1/3}\left(\frac{\alpha}{10^{-2}}\right)^{2/3}\left(\frac{\Sigma_a}{100\ \mathrm{g\ cm^{-2}}}\right)^{4/3}\kappa_0^{2/3}\ \mathrm{AU}\ . \tag{26}$$

The mass flux inside R_{s-i} is larger than that outside. Subtracting the two,

$$\Delta\dot{M} = -11 \times 10^{-7}\left(\frac{\alpha}{10^{-2}}\right)^2\left(\frac{\Sigma_a}{100\ \mathrm{g\ cm^{-2}}}\right)^3\kappa_0\ M_\odot\ \mathrm{yr}^{-1}\ . \tag{27}$$

Thus material will gradually be depleted over a range in radius around R_{s-i}. Since this depletion cannot be sustained indefinitely, the disk structure will be time-dependent. It will evolve toward a time-independent solution in which the layered ice-sublimation opacity solution is joined to a constant-$\dot{M}$ ice sublimation opacity solution, which is joined to a constant-$\dot{M}$ ice grain opacity solution, which in turn is joined to a layered ice grain opacity solution. The outer boundary of the layered ice-sublimation opacity zone is then set by the condition that the mass flux is equal to the mass flux available from the outer disk.

Finally, consider the spectral energy distribution of the layered disk model. Because the mass flux increases outward in the disk, the effective temperature profile is $T_e \sim r^{-1/2}$ outside

of 0.1 AU, which differs from the canonical $T_e \sim r^{-3/4}$ expected for a constant mass flux disk. The effective temperature profile is directly related to the spectral energy distribution of the disk. For the canonical constant mass flux model $\lambda F_\lambda \sim \lambda^{-4/3}$ (Lynden-Bell & Pringle 1974), while for a disk with $T_e \sim r^{-1/2}$ throughout, $\lambda F_\lambda \sim$ const. The full spectral energy distribution will be the sum of that due to a constant mass flux disk inside 0.1 AU and a layered solution outside; the effective temperature at the transition radius is ≈ 300 K, so the layered solution begins to dominate the spectral energy distribution at about $\lambda \simeq 0.37hc/kT_e \simeq 15$ μm. Thus, ignoring reprocessing of stellar radiation, we expect that $\lambda F_\lambda \sim \lambda^{-4/3}$ at $\lambda \lesssim 15$ μm and $\lambda F_\lambda \sim \lambda^0$ at longer wavelength.

We have calculated the emergent spectrum from our layered model, and the result is shown in Figure 2. Only the disk emission is shown; the boundary layer and star are not included, nor is reprocessed light taken into account. The disk is assumed to be face-on at a distance of 100 pc. It extends from 2.5 $R_\odot$ to 28 AU, where the accretion rate is 4.1×10^{-7} $M_\odot$ yr^{-1}. The disk is truncated at 28 AU because at larger radii the layered accretion solution is gravitationally unstable (see the Appendix). Notice that, as expected, the spectrum becomes flat longward of about 20 μm. This is consistent with the observed average flattening of T Tauri stars at about this wavelength (see Fig. 9 of Kenyon & Hartmann 1995), although it cannot account for all the infrared excess in sources that have a flat spectrum from 1 μm longward (see, e.g., Adams, Lada, & Shu 1988).

4. CONCLUSION

As a final word of explanation, it may be helpful to consider how the layered model evolves in time. We begin with a quiescent nebula with mass distribution $\Sigma(r)$. We assume there is a small residual field in the disk, so that it is Balbus-Hawley unstable. Within a few orbital periods, the instability saturates, the surface layers of the disk become turbulent, and a layered solution is established. In some regions of the disk the surface density may be small enough that the entire thickness of the disk is active. These regions will become layered if their surface density rises above $2\Sigma_a$; the precise evolution of the surface density depends on the initial conditions. Other regions can lose surface density and become unlayered. As the disk evolves material accumulates in the dead zone at $r \lesssim 6$ AU. This happens independent of the initial conditions, since the mass flux into the inner disk is governed by the layered solution at larger radius. The accumulation of matter in the dead zone cannot continue indefinitely, and an instability (e.g., gravitational instability) will activate part of the dead zone after a period of 10^4–10^5 yr. The layered solution is invalid during the subsequent event, but presumably the disk will return to a layered state after enough of the dead zone has been accreted to make it stable again. Thus T Tauri disks should spend a large fraction of their lives in a layered state.

To summarize our results, then, the layered accretion model presented here accounts naturally for some characteristic features of accretion in T Tauri systems. It predicts an accretion rate comparable to what is inferred from observations. It also predicts a buildup of surface density in the disk at a fraction of an AU, comparable to what is required to fuel FU Orionis outbursts. A related feature of the model is that it predicts a rather slow fall-off in effective temperature with radius, similar to what is required to fit the observed spectral energy distribution of some T Tauri stars. Finally, the model has a sound physical motivation in the theory of angular momentum transport by turbulence initiated by the MHD instability of Balbus & Hawley.

Several ingredients of our model are now uncertain, but could improve significantly with additional theoretical effort. Among the leading uncertainties is the magnitude of the angular momentum flux inside the active layer. Numerical simulation of MHD turbulence in disks (HGB1; HGB2) provide some support for the model used here, but they do not specifically address the evolution of a system with significant resistivity. Three-dimensional simulations of a stratified disk with vertically varying resistivity are now practical and might provide a better prescription for angular momentum transport in the active layer.

The crude one-zone models for the vertical structure of the disk used to derive our analytic layered accretion solutions could easily be improved on. Our model, for example, does not take account of vertical energy transport by convection. The approximation that $\Sigma_a \simeq$ the cosmic-ray stopping length is also crude, and could be improved on with a detailed vertical structure model that self-consistently calculates the variation of electron fraction with height.

Another important source of uncertainty is dust. It controls both the opacity and potentially the recombination rate in T Tauri disks. While the development of a predictive theory for the dust size spectrum appears to be still very difficult, it should, however, be possible to better quantify which size spectra are consistent with a layered accretion disk model.

I am grateful to Steve Balbus, Lee Hartmann, John Hawley, Ramesh Narayan, Eve Ostriker, Jim Stone, and Insu Yi for their encouragement and suggestions. This work was supported by NASA grant NAG 5-2837.

APPENDIX

WATER ICE AND ICE SUBLIMATION OPACITY REGIMES

In the ice-sublimation opacity regime, $167 < T_c < 203$, the opacity is $\kappa = 2 \times 10^{16} \kappa_0 T^{-7}$ cm^2 g^{-1} according to the analytic fit of Bell & Lin (1994). Then the layered accretion solution is

$$T_c = 222 \left(\frac{r}{1\ \mathrm{AU}}\right)^{-3/20} \left(\frac{M}{1\ M_\odot}\right)^{1/20} \left(\frac{\alpha}{10^{-2}}\right)^{1/10} \left(\frac{\Sigma_a}{100\ \mathrm{g\ cm^{-2}}}\right)^{1/5} \kappa_0^{1/10}\ \mathrm{K}\,, \tag{28}$$

$$T_e = 95.8 \left(\frac{r}{1\ \mathrm{AU}}\right)^{-33/80} \left(\frac{M}{1\ M_\odot}\right)^{11/80} \left(\frac{\alpha}{10^{-2}}\right)^{11/40} \left(\frac{\Sigma_a}{100\ \mathrm{g\ cm^{-2}}}\right)^{3/10} \kappa_0^{1/10}\ \mathrm{K}\,, \tag{29}$$

$$\dot{M} = 1.18 \times 10^{-7} \left(\frac{r}{1\ \mathrm{AU}}\right)^{27/20} \left(\frac{M}{1\ M_\odot}\right)^{-9/20} \left(\frac{\alpha}{10^{-2}}\right)^{11/10} \left(\frac{\Sigma_a}{100\ \mathrm{g\ cm^{-2}}}\right)^{6/5} \kappa_0^{1/40}\ M_\odot\ \mathrm{yr}^{-1}\,, \tag{30}$$

$$\rho = 1.92 \times 10^{-10}\left(\frac{r}{1\ \mathrm{AU}}\right)^{-57/40}\left(\frac{M}{1\ M_\odot}\right)^{19/40}\left(\frac{\alpha}{10^{-2}}\right)^{-1/20}\left(\frac{\Sigma_a}{100\ \mathrm{g\ cm^{-2}}}\right)^{9/10}\kappa_0^{-1/20}\ \mathrm{g\ cm^{-3}}\ . \tag{31}$$

Because of the steep temperature dependence of the opacity, the layered model is only weakly dependent on κ_0.

Assuming that radiative recombination is the dominant recombination pathway, the magnetic Reynolds number at the base of the active layer is

$$Re_M = 0.36\left(\frac{r}{1\ \mathrm{AU}}\right)^{81/40}\left(\frac{M}{1\ M_\odot}\right)^{-27/40}\left(\frac{\alpha}{10^{-2}}\right)^{3/20}\left(\frac{\Sigma_a}{100\ \mathrm{g\ cm^{-2}}}\right)^{-1/5}\kappa_0^{3/20}\ , \tag{32}$$

consistent with the gas being well coupled to the field at the base of the radiative layer.

The inner boundary of the ice sublimation opacity zone lies at

$$R_{\mathrm{in}} = 1.8\left(\frac{M}{1\ M_\odot}\right)^{1/3}\left(\frac{\alpha}{10^{-2}}\right)^{2/3}\left(\frac{\Sigma_a}{100\ \mathrm{g\ cm^{-2}}}\right)^{4/3}\kappa_0^{2/3}\ \mathrm{AU}\ , \tag{33}$$

while the outer boundary is at

$$R_{\mathrm{out}} = 6.6\left(\frac{M}{1\ M_\odot}\right)^{1/3}\left(\frac{\alpha}{10^{-2}}\right)^{2/3}\left(\frac{\Sigma_a}{100\ \mathrm{g\ cm^{-2}}}\right)^{4/3}\kappa_0^{2/3}\ \mathrm{AU}\ . \tag{34}$$

The outer boundary of the layered accretion solution may be smaller than this if there is an insufficient mass flux at the outer boundary.

For $T_c < 167$ K the main contribution to the opacity is from water ice grains, which give $\kappa = 2 \times 10^{-4}\kappa_0 T^2$. Then the layered accretion solution is

$$T_c = 2850\left(\frac{r}{1\ \mathrm{AU}}\right)^{-3/2}\left(\frac{M}{1\ M_\odot}\right)^{1/2}\left(\frac{\alpha}{10^{-2}}\right)\left(\frac{\Sigma_a}{100\ \mathrm{g\ cm^{-2}}}\right)^{2}\kappa_0\ \mathrm{K}\ , \tag{35}$$

$$T_e = 181\left(\frac{r}{1\ \mathrm{AU}}\right)^{-3/4}\left(\frac{M}{1\ M_\odot}\right)^{1/4}\left(\frac{\alpha}{10^{-2}}\right)^{1/2}\left(\frac{\Sigma_a}{100\ \mathrm{g\ cm^{-2}}}\right)^{3/4}\kappa_0^{1/4}\ \mathrm{K}\ , \tag{36}$$

$$\dot{M} = 4.1 \times 10^{-7}\left(\frac{\alpha}{10^{-2}}\right)^{2}\left(\frac{\Sigma_a}{100\ \mathrm{g\ cm^{-2}}}\right)^{3}\kappa_0\ M_\odot\ \mathrm{yr^{-1}}\ , \tag{37}$$

$$\rho = 5.4 \times 10^{-11}\left(\frac{r}{1\ \mathrm{AU}}\right)^{-3/4}\left(\frac{M}{1\ M_\odot}\right)^{1/4}\left(\frac{\alpha}{10^{-2}}\right)^{-1/2}\kappa_0^{-1/2}\ \mathrm{g\ cm^{-3}}\ . \tag{38}$$

Because the opacity scales as T^2, $\dot{M}$ is independent of r.

The magnetic Reynolds number at the base of the active layer is

$$Re_M = 17\left(\frac{\alpha}{10^{-2}}\right)^{3/2}\left(\frac{\Sigma_a}{100\ \mathrm{g\ cm^{-2}}}\right)^{5/2}\kappa_0^{3/2}\ , \tag{39}$$

again consistent with the gas being well coupled to the magnetic field.

Recall that a thin gaseous disk is subject to a linear, axisymmetric gravitational instability if Toomre's parameter $Q \equiv c\Omega/\pi G\Sigma < 1$. In the water ice opacity zone Q is, assuming $\Sigma_d = 0$,

$$Q = 1800\left(\frac{r}{1\ \mathrm{AU}}\right)^{-9/4}\left(\frac{M}{1\ M_\odot}\right)^{3/4}\left(\frac{\alpha}{10^{-2}}\right)^{1/2}\kappa_0^{1/2}\ . \tag{40}$$

Clearly Q drops rapidly with r. It reaches 1 at

$$R = 28\left(\frac{M}{1\ M_\odot}\right)^{1/3}\left(\frac{\alpha}{10^{-2}}\right)^{2/9}\kappa_0^{2/9}\ \mathrm{AU}\ , \tag{41}$$

independent of Σ_a. It seems likely, therefore, that in the outer regions of the disk density waves will also contribute to the angular momentum flux, thereby increasing the accretion rate.

REFERENCES

Adams, F. C., Lada, C. J., & Shu, F. H. 1988, ApJ, 326, 865
Balbus, S. A., & Hawley, J. F. 1991, ApJ, 376, 214 (BH)
Balbus, S. A., Hawley, J. F., & Stone, J. M. 1995, in preparation
Basri, G., & Bertout, C. 1989, ApJ, 341, 340
Bell, K. R., & Lin, D. N. C. 1994, ApJ, 477, 987
Brandenburg, A., Nordlund, A., Stein, R., & Torkelsson, U. 1995, ApJ, 446, 741
Cameron, A. G. W. 1978, Moon & Planets, 18, 5
Christodoulou, D. M., & Narayan, R. 1992, ApJ, 388, 451
Dolginov, A. Z., & Stepinski, T. F. 1994, ApJ, 427, 377
Dubrulle, B. 1992, A&A, 266, 592
Glassgold, A. E., Lucas, R., & Omont, A. 1986, A&A, 157, 35
Hartmann, L., & Kenyon, S. 1990, ApJ, 349, 190
Hartmann, L., Kenyon, S., & Hartigan, P. 1993, in Protostars and Planets III, ed. E. H. Levy & J. Lunine (Tucson: Univ. Arizona Press), 497
Hawley, J. F., Gammie, C. F., & Balbus, S. A. 1995a, ApJ, 440, 742 (HGB1)
———. 1995b, ApJ, in preparation (HGB2)
Hayashi, C. 1981, Prog. Theor. Phys., 70, 35
Hubeny, I. 1990, ApJ, 351, 632
Jokipii, J. R. 1991, in Sun in Time, ed. C. P. Sonett, M. S. Giampapa, & M. S. Matthews (Tucson: Univ. Arizona Press), 205
Kenyon, S. J., & Hartmann, L. 1995, ApJS, 101, 117
Königl, A. 1995, in Research Trends in Plasma Astrophysics, AIP Press, in press
Lin, D. N. C., & Papaloizou, J. 1980, MNRAS, 191, 37

Lynden-Bell, D., & Pringle, J. E. 1974, MNRAS, 168, 603
Mathis, J. S., Rumpl, W., & Nordsieck, K. H. 1977, ApJ, 217, 425
Montmerle, T., Feigelson, E. D., Bouvier, J., & Andre, P. 1993, in Protostars and Planets III, ed. E. H. Levy & J. Lunine (Tucson: Univ. Arizona Press), 689
Paczyński, B. 1976, Comm. Astrophys., 6, 95
Pollack, J. B., McKay, C. P., & Christofferson, B. M. 1985, Icarus, 64, 471
Ryu, D., & Goodman, J. 1992, ApJ, 388, 438
Shakura, N. I., & Sunyaev, R. A. 1973, A&A, 24, 337
Shakura, N. I., Sunyaev, R. A., & Zilitinkevich, S. S. 1978, A&A, 62, 179
Spitzer, L., & Tomasko, M. G. 1968, ApJ, 152, 971
Stepinski, T. F. 1992, Icarus, 97, 130
Stone, J. M., & Balbus, S. A. 1995, ApJ, submitted
Umebayashi, T. 1983, Prog. Theor. Phys., 69, 480
Umebayashi, T., & Nakano, T. 1981, PASJ, 33, 617
Weidenschilling, S. J., & Cuzzi, J. N. 1993, in Protostars and Planets III, ed. E. H. Levy & J. Lunine (Tucson: Univ. Arizona Press), 1031
Zahn, J.-P. 1991, in Structure and Emission Properties of Accretion Disks, ed. C. Bertout et al. (Gif sur Yvette: Edi. Frontieres), 87